

# An Analytical Model for the Lift on an Inline Oscillating Cylinder under No Resonance Condition

Shaikh Jaweed<sup>1</sup>, Dr. Krishna Prasad<sup>2</sup>

<sup>1</sup>(Department of Humanities and Sciences, M. H. Saboo Siddik College of Engg./Mumbai University, India)

<sup>2</sup>(Department of Mathematics, M. J. College, Jalgaon/ North Maharashtra University, India)

---

**Abstract:** An analytical model under the no resonance condition is developed to determine the lift on inline oscillating circular cylinder under the lock-on regime. From numerical simulations of the flow field, lift coefficient data are obtained over the inline oscillating circular cylinder. Spectral analysis is applied to the data to characterize the non-linear coupling between the vortex shedding frequency and its third harmonic. From this analysis it is concluded that the van der Pol equation should be used to model the lift coefficient on inline oscillating circular cylinder in the lock-on regime.

**Keywords:** Inline oscillations, circular cylinder, Lift, Higher order spectra, auto-bispectra, auto-trispectra, Non-linear coupling, no resonance

---

## I. Introduction

Drag and lift forces on circular cylinder are directly related to the vortex shedding pattern in their wakes. Reducing these forces, reducing vortex induced-vibrations or augmenting the lift component would be the area of interest. To affect the wake pattern and associated forces on the circular cylinder, different forcing conditions have been shown significantly and one such condition is oscillation forcing. Studies by Tokumaru and Dimostakis [1], Lu and Sato [2], and Chou [3] on rotationally oscillating cylinder showed a significant drag reduction under specific forcing conditions. Choi et al. [4] showed that the maximum amplitude of the lift coefficient is increased in the lock-on region.

The optimal approach to assess effects of cylinder forcing on the wake structure and the lift and drag forces would be a time-domain numerical simulation of the fluid flow and the structure's motion. On the other hand, and for different purposes such as optimization of the forcing parameters, analytical models have been proposed as a more efficient alternative for determining fluctuating forces on oscillating circular cylinder. One of the first models proposed for vortex-induced vibrations of circular cylinder is the one by Hartlen and Currie [5]. In that model, the lift presented by Rayleigh equation, is linearly coupled to the cylinder's motion. Using a combination of approximate solutions of the Rayleigh and Van der Pol equations and amplitude and phase measurements of higher-order spectral moments, Nayfeh, Owis and Hajj [6] showed that the lift coefficient, on the stationary circular cylinders should be modeled by the self-excited Van der Pol equation. Isam Janajreh and Muhammad Hajj [7] also proved the same result for the lift coefficient, on rotationally oscillating cylinder under the resonance condition. The extension of such models to develop an analytical model for the lift force on inline oscillating circular cylinder would be very beneficial for modeling vortex-induced vibrations, drag reduction or lift augmentation.

In this model we have determined an analytical model for the prediction of the lift on inline oscillating circular cylinder under no resonance condition. Numerical simulations are performed to generate a data base from which parameters for the developed model are determined. Amplitude and phase measurements from higher order spectral parameters are matched with approximate solutions of the model to characterize the nonlinearities in the model and determine these parameters.

## II. CFD Simulations

Direct Numerical simulations of the unsteady incompressible Navier-Stokes equations for different cases of the flow over an oscillating circular cylinder were performed. All simulations were performed at  $Re = U_{\infty} D / \nu = 100$ . The computational domain extended 5 cylinder diameters upstream, 10 diameters cross-stream on each side and 20 diameters down-stream. The domain was staggered by multiple blocks with a quadratic cell type mesh, in order to provide more faces and to enhance the cell communication and computational accuracy. The cylinder wall was padded with a boundary layer mesh to accurately capture the

viscous layer. The first cell thickness is  $0.0002D$  and with a linear growth rate of 1.05. Imposed cylinder rotations were determined by two parameters, namely, the non-dimensional amplitude,  $\dot{\theta}_{\max} D / 2U_{\infty} = 0.5$  where  $\dot{\theta}_{\max}$  is the maximum forcing angular velocity, and the forcing frequency  $f_f D / U_{\infty} = 0.1$ , where  $f_f$  is the dimensional forcing frequency.

### 2.1 Spectral Analysis

Traditional signal processing techniques used in data analysis are based on second-order statistics, such as the power spectra which are the Fourier transforms of the second-order correlation functions. These quantities yield an estimate of energy content of the different frequency components in a signal or the coherence between equal frequency components in two signals. In many cases, higher-order spectral moments can be used to obtain more information from signals or time series. In nonlinear systems, frequency components interact to pass energy to other components at their sum and/or difference frequency. Because of this interaction, the phases of the interacting components are coupled. This phase coupling can be used for the detection of nonlinear interactions between frequency components in one or more time series. Faced with an unknown system in terms of its nonlinear characteristic, these moments can be applied to identify quadratic and cubic nonlinearities. The bi-spectrum [8, 9, 10], which is the next higher order spectrum to power spectrum, has been established as a tool to quantify the level of phase coupling among three frequency components and thus identify quadratic nonlinearities. To this work our particular interest is the tri-spectrum [11], which is the next higher order moment to the bi-spectrum, and which is used to detect and characterize cubic nonlinearities expected to be a part of the lift coefficient.

Above introduced higher order spectral moments are multi-dimensional Fourier Transforms of higher-order statistical moments. For any real random process  $x(t)$  and its stationary moments up to order  $n$ , one could define the  $n^{\text{th}}$  order moment function as

$$m_n(\tau_1, \tau_2, \dots, \tau_{n-1}) = E\{x(t)x(t + \tau_1)\dots x(t + \tau_{n-1})\} \quad (1)$$

Where  $E\{ \}$  represents ensemble averaging and  $\tau_1, \tau_2, \dots, \tau_{n-1}$  represents time differences.

By Fourier Transforming the second, third and fourth-order moment functions, one obtains, respectively, the auto-power spectrum, auto-bispectrum and auto-trispectrum [11]. Then the hierarchy of higher-order moment spectra is expressed as

$$S_{xx}(f) = \lim_{T \rightarrow \infty} \frac{1}{T} E[X_T^*(f)X_T(f)] \quad (2)$$

$$S_{xxx}(f_1, f_2) = \lim_{T \rightarrow \infty} \frac{1}{T} E[X_T^*(f_1)X_T^*(f_2)X_T(f_1 + f_2)] \quad (3)$$

$$S_{xxxx}(f_1, f_2, f_3) = \lim_{T \rightarrow \infty} \frac{1}{T} E[X_T^*(f_1)X_T^*(f_2)X_T^*(f_3)X_T(f_1 + f_2 + f_3)] \quad (4)$$

Where  $X_T(f)$  is the Fourier Transform of  $x(t)$  define over a time duration  $T$ , and the superscript  $*$  is used to denote complex conjugate. The higher-order spectral moments and their normalized counterparts are capable of identifying nonlinear coupling among frequency components and quantifying their phase relations [8, 9,10]. In this work, we will stress the use of the auto-trispectrum to determine the phase relation between the vortex shedding component and its third harmonic. This relation will be used in determining the parameters of the proposed analytical model.

### III. Analytical Model for the Lift

The lift coefficient on inline oscillating cylinder is modeled by a parametrically excited van der Pol oscillator which is written as

$$\ddot{C}_L + \omega_s^2 C_L^2 - \mu_v \dot{C}_L + \alpha_v C_L^2 \dot{C}_L + \xi \cos(\Omega t + \tau) C_L = 0 \quad (5)$$

Where  $\omega_s$  is the shedding frequency,  $\mu_v$  and  $\alpha_v$  represents the linear and nonlinear damping coefficients,  $\xi$  and  $\tau$  are respectively the amplitude and phase of the external harmonic function which represents the inline

oscillations. To balance the damping, nonlinearities and parametric excitation in equation (5),  $\mu_v$ ,  $\alpha_v$  and  $\xi$  are scaled as  $\epsilon\mu_v$ ,  $\epsilon\alpha_v$  and  $\epsilon\xi$ . The parametrically excited van der Pol equation is then written as

$$\ddot{C}_L + \omega_s^2 C_L^2 - \epsilon\mu_v \dot{C}_L + \epsilon\alpha_v C_L^2 \dot{C}_L + \epsilon\xi \cos(\Omega t + \tau) C_L = 0 \quad (6)$$

Using the method of multiple scales [12, 13], an analytical approximate solution is derived for equation (6) for the no-resonance condition, i.e.  $\Omega$  is away from  $2\omega_s$ . The approximate solution is of the form

$$C_L(t) \approx a \cos(\omega_s t + \beta) + \frac{a^3 \alpha_v}{32\omega_s} \cos\left(3(\omega_s t + \beta) + \frac{\pi}{2}\right) + \frac{a\xi}{(2\omega_s - \Omega)2\Omega} \cos((\Omega - \omega_s)t + \tau - \beta + \pi) + \frac{a\xi}{(2\omega_s + \Omega)2\Omega} \cos((\Omega + \omega_s)t + \tau + \beta) \quad (7)$$

In Equation (7), the amplitude  $a$  and phase  $\beta$  are governed by

$$\dot{a} = \frac{\mu_v}{2} a - \frac{\alpha_v}{8} a^3 \text{ and } \dot{\beta} = 0 \quad (8)$$

When  $a$  and  $\beta$  are constants in equation (8), i.e., for steady-state oscillations, the solution given in equation (7) represents a periodic motion which can be written in complex form as

$$C_L(t) \approx \frac{a}{2} \left\{ e^{i(\omega_s t + \beta)} + e^{-i(\omega_s t + \beta)} \right\} + \frac{a^3 \alpha_v}{64\omega_s} \left\{ e^{3i(\omega_s t + \beta) + i\frac{\pi}{2}} + e^{-3i(\omega_s t + \beta) - i\frac{\pi}{2}} \right\} + \frac{a\xi}{(2\omega_s - \Omega)4\Omega} \left\{ e^{i[(\Omega - \omega_s)t + \tau - \beta + \pi]} + e^{-i[(\Omega - \omega_s)t + \tau - \beta + \pi]} \right\} + \frac{a\xi}{(2\omega_s + \Omega)4\Omega} \left\{ e^{i[(\Omega + \omega_s)t + \tau + \beta]} + e^{-i[(\Omega + \omega_s)t + \tau + \beta]} \right\} \quad (9)$$

The Fourier transform  $L(\omega)$  of  $C_L(t)$  is then given by

$$C_L(t) \approx \frac{a}{2} \left\{ e^{i\beta} \delta(\omega - \omega_s) + e^{-i\beta} \delta(\omega + \omega_s) \right\} + \frac{a^3 \alpha_v}{64\omega_s} \left\{ e^{3i\beta + i\frac{\pi}{2}} \delta(\omega - 3\omega_s) + e^{-3i\beta - i\frac{\pi}{2}} \delta(\omega + 3\omega_s) \right\} + \frac{a\xi}{(2\omega_s - \Omega)4\Omega} \left\{ e^{i(\tau - \beta + \pi)} \delta(\omega + \omega_s - \Omega) + e^{-i(\tau - \beta + \pi)} \delta(\omega - \omega_s + \Omega) \right\} + \frac{a\xi}{(2\omega_s + \Omega)4\Omega} \left\{ e^{i(\tau + \beta)} \delta(\omega - \omega_s - \Omega) + e^{-i(\tau + \beta)} \delta(\omega + \omega_s + \Omega) \right\} \quad (10)$$

Examining the expression for  $L(\omega)$  given in equation (10), it is noted that the solution thus contains components with frequencies at  $\omega_s$ ,  $3\omega_s$ ,  $\Omega - \omega_s$  and  $\Omega + \omega_s$ . The amplitudes and phases of these components are given by

$$L(\omega_s) = \frac{1}{2} a e^{i\beta} \quad (11)$$

$$L(3\omega_s) = \frac{a^3 \alpha_v}{64\omega_s} e^{3i\beta + i\frac{\pi}{2}} \quad (12)$$

$$L(\Omega - \omega_s) = \frac{a\xi}{(2\omega_s - \Omega)4\Omega} e^{i(\tau - \beta + \pi)} \quad (13)$$

$$L(\Omega + \omega_s) = \frac{a\xi}{(2\omega_s + \Omega)4\Omega} e^{i(\tau + \beta)} \quad (14)$$

The auto-trispectrum is then used to identify different frequency components in the above solution. Two of these moments are

$$S_{III}(\omega_s, \omega_s, \omega_s) \approx \frac{a^6 \alpha_v}{512} e^{i\frac{\pi}{2}} \quad (15)$$

$$S_{III}(\Omega - \omega_s, \omega_s, \omega_s) \approx \frac{a^4 \xi^2}{64\Omega^2 (2\omega_s - \Omega)(2\omega_s + \Omega)} e^{-i\pi} \quad (16)$$

The magnitude of the auto-trispectrum  $S_{III}(\omega_s, \omega_s, \omega_s)$  depends on the coefficient of the cubic nonlinearity  $\alpha_v$ . Its phase, given by  $\phi(3\omega_s) - 3\phi(\omega_s)$ , is equal to  $\pi/2$ . The magnitude of the auto-trispectrum  $S_{III}(\Omega - \omega_s, \omega_s, \omega_s)$  depends on the coefficient of the parametric excitation  $\xi$ . Its phase is equal to  $-\pi$ . For nonlinear systems that can be modeled by the parametrically excited van der Pol equation, these quantities can be used to determine  $\alpha_v$  and  $\xi$  and determine the suitability of using the harmonically-excited van der Pol equation to model the lift on a forced inline oscillating cylinder. For the parametrically excited van der Pol equation with no resonance, the steady state oscillations are obtained by setting  $\dot{a} = 0$  in equation (8). Under those conditions, the amplitude of the vortex shedding frequency component,  $a$ , is related to the damping and nonlinear damping coefficients by

$$a = 2\sqrt{\frac{\mu_v}{\alpha_v}} \quad (17)$$

To determine linear and nonlinear damping coefficients, and the excitation parameter in equation (6) from the amplitude and phases of the Fourier components in the time series, the lift coefficient is re-written as

$$C_L(t) \approx a_1 \cos(\omega_s t + \beta) + a_2 \cos((\Omega - \omega_s)t + \tau - \beta + \pi) + a_3 \cos\left(3(\omega_s t + \beta) + \frac{\pi}{2}\right) + a_4 \cos((\Omega + \omega_s)t + \tau + \beta) \quad (18)$$

By comparing equation (18) with equation (7) and applying equation (17), one obtains

$$\alpha_v = \frac{32\omega_s a_3}{a_1^3} \quad (19)$$

$$\mu_v = \frac{1}{4} \alpha_v a_1^2 \quad (20)$$

$$\xi = \frac{a_2(2\omega_s - \Omega)2\Omega}{a_1} \quad (21)$$

$$\text{or } \xi = \frac{a_4(2\omega_s + \Omega)2\Omega}{a_1} \quad (22)$$

Alternatively, and as explained above,  $\alpha_v$  and  $\xi$  can be obtained from the magnitude of the auto-trispectra defined in equations (15) and (16). Rearranging equations (15) and (16), one obtains

$$\alpha_\alpha = \frac{512\omega_s |S_{III}(\omega_s, \omega_s, \omega_s)|}{a^6} \quad (23)$$

And

$$\xi = \sqrt{\frac{64\Omega^2(2\omega_s - \Omega)(2\omega_s + \Omega) |S_{III}(\Omega - \omega_s, \omega_s, \omega_s)|}{a^4}} \quad (24)$$

Using the Fourier transform of  $C_L(t)$  at frequencies  $\Omega - \omega_s, \Omega + \omega_s$  and  $\omega_s$ , the phase of parametric excitation can be determine as

$$\tau = \Phi(L(\Omega - \omega_s)) + \Phi(L(\omega_s)) - \pi \quad (25)$$

$$\text{or } \tau = \Phi(L(\Omega + \omega_s)) - \Phi(L(\omega_s)) \quad (26)$$

Where  $\Phi(L(\omega_s))$  is the phase angle of  $L(\omega_s)$ ,  $\Phi(L(\Omega - \omega_s))$  is the phase angle of  $L(\Omega - \omega_s)$  and  $\Phi(L(\Omega + \omega_s))$  is the phase angle of  $L(\Omega + \omega_s)$ .

#### IV. Results and Discussion

Vorticity contours in the wake of the cylinder subjected to inline oscillations under no resonance conditions are presented in Fig.1. The vortex shedding pattern presented in this Fig.1 is compared with the pattern observed when the cylinder is held stationary as presented in Fig. 2. Vortex shedding patterns observed in both the cases are nearly similar.

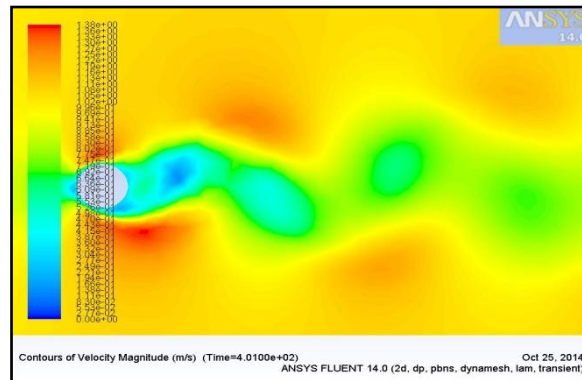


**Figure 1:** Vorticity contour in the wake of inline oscillating cylinder. Forcing condition:  $\dot{\theta}_{\max} D/2U_\infty = 0.01, f_s D/U_\infty = 0.4$

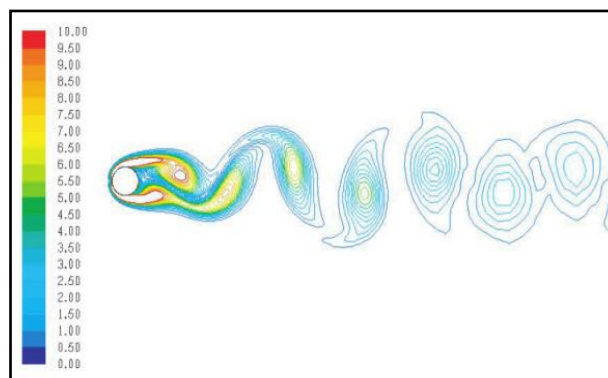


**Figure 2:** Vorticity contour in the wake of stationary cylinder. Forcing condition:  $St = f_s D/U_\infty = 0.1747$  (adapted from Isam Janajreh and Muhammad Hajj [7])

The above notion is further strengthened by the lift and drag time series in the lock-on case, presented in Fig.3. Both coefficients are characterized by perfect sinusoidal variations. The lift has a major frequency that corresponds to the vortex shedding frequency. The major frequency component in the drag is twice that of the lift. This sinusoidal behavior indicates a perfect vortex shedding as would be observed in the stationary case.

To verify the lift coefficient model, the lift spectral parameters and lift model parameters in parametrically excited van der Pol equation are obtained from the power spectra. In this CFD simulation post-processing (Fast Fourier Transform, FFT) was performed in Ansys fluent, Tecplot-360 and Matlab for the graph of power spectra. And then result from the Matlab software was used to identify lift spectral parameters.

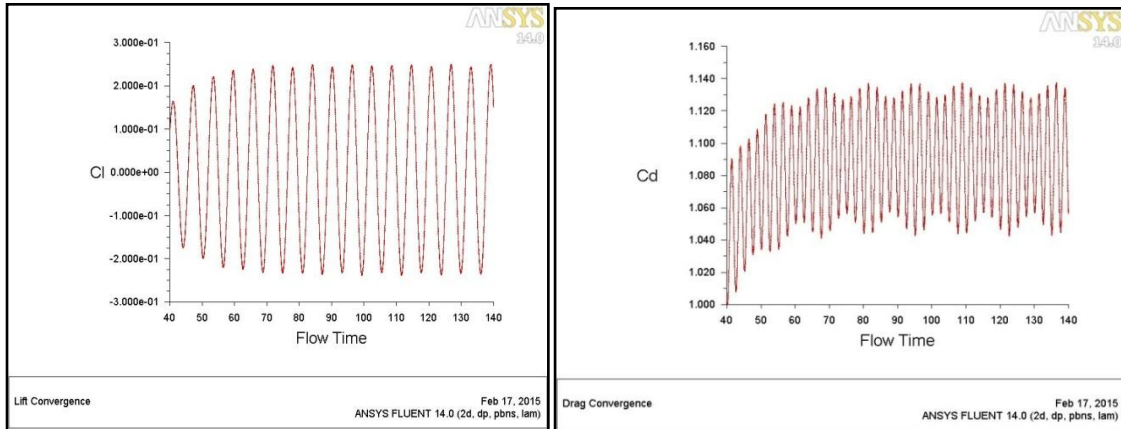


**Figure 3:** Time histories of the lift and drag coefficients on the inline oscillating cylinder. Forcing condition:  $\dot{\theta}_{\max} D / 2U_{\infty} = 0.01$ ,  $f_f D / U_{\infty} = 0.4$

The power spectrum of the lift coefficient on the inline oscillating cylinder, obtained from the CFD simulations at an excitation frequency of 0.4 Hz and amplitude near 0.01 is shown in figure 5. In this figure, peaks at  $\omega_s, 3\omega_s, \Omega - \omega_s$  and  $\Omega + \omega_s$  are noted. These peaks show that there is no resonance under these conditions. Values of the spectral parameters  $f, a_1, a_2, a_3, a_4, \Phi(L(\omega_s)), \Phi(L(\Omega - \omega_s))$  and  $\Phi(L(\Omega + \omega_s))$  are shown in Table 1. These values are then used to estimate  $\xi, \tau, \mu_v$  and  $\alpha_v$  based on equations 19, 20, 21 and 24. These parameters are given in Table 2. They can be used to predict the steady-state lift by integrating equation 5.

**Table 1.** Lift spectral parameters for the inline oscillating cylinder (no resonance case)

$\Omega$	0.4
y/D	0.01
f	0.1633
$a_1$	0.17
$a_2$	0.004
$a_3$	0.0005
$a_4$	0.0012
$\Phi(L(\omega_s))$	1.84
$\Phi(L(\Omega - \omega_s))$	3.525
$\Phi(L(\Omega + \omega_s))$	3.33

**Table 2:** Lift model parameters in parametrically excited van der Pol equation (no resonance case)

$\Omega$	0.4
y/D	0.01
$\xi$ from $L(\Omega - \omega_s)$	0.0311
$\xi$ from $L(\Omega + \omega_s)$	0.0138
$\tau$ (rad)	2.225
$\mu_v$	0.0242
$\alpha_v$ from $L(3\omega_s)$	3.3469

Validation of the analytical model and its parameters is demonstrated by comparing its integrated time series with the one obtained from the original numerical simulation. This comparison is presented in Fig.4. Obviously, the derived model predicts the sinusoidal characteristic of the vortex shedding. The difference observed at the high frequencies is relatively insignificant when comparing it with the spectral amplitudes of the vortex shedding frequency. This difference may be due to the level of accuracy in the integration of the analytical model. Comparison of the two time series in Fig.4 shows that the identified parameters can be used to correctly determine the amplitude variations in the lift time series.

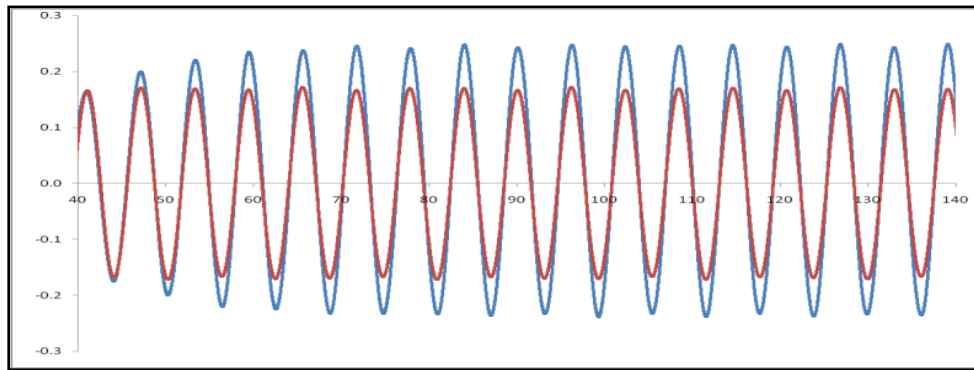


**Figure 4:** Comparison of the analytically modeled (red line) and numerically simulated (blue line) lift time series

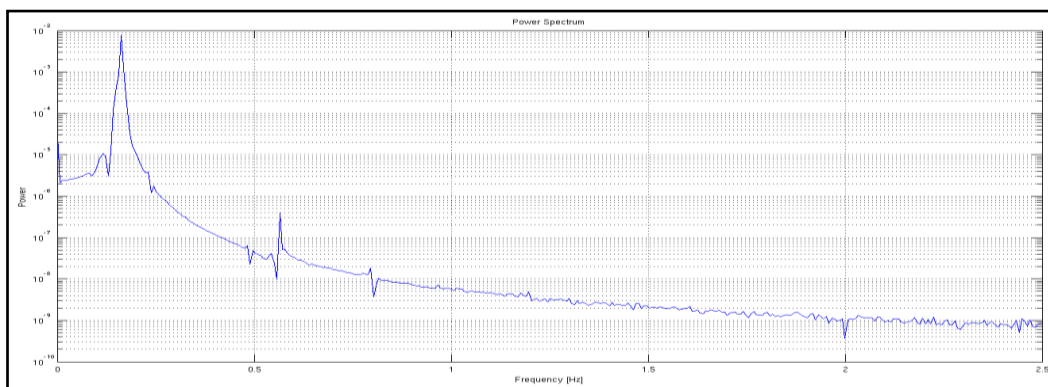


**Figure 5:** The power spectra of the numerically simulated lift coefficients obtained from Matlab Software

## V. Conclusion

In this study, an analytical model for the prediction of the lift on an inline oscillating cylinder in the lock-on regime has been developed. The parameters of the developed model were determined from a numerical simulation of the flow field using higher-order spectral analysis of the lift data. Higher-order spectral analysis of the lift data yielded relevant quantities that were matched with approximate solutions of the assumed model. Fast Fourier Transform (FFT) was performed using Matlab. The validity of the model has been demonstrated by comparing time domain characteristics of the analytically modeled lift coefficient with the numerically simulated data. Numerical simulation using Ansys fluent software is performed to validate the analytical model for the lift on an inline oscillating cylinder under no resonance. The perfect matching of the lift time series shows that Van der Pol oscillator should be used to model the lift on an inline oscillating cylinder.

## References

- [1]. P. T. Tokumaru, and P. E. Dimotakis, Rotary oscillation control of a cylinder wake. *J. Fluid Mech.*, 224(77), 1991.
- [2]. X.-Y. Lu and J. Sato. A numerical study of flow past a rotationally oscillating circular cylinder. *J. Fluids Struct.*, 10, 829, 1996.
- [3]. M.-H. Chou. Synchronization of vortex shedding from a cylinder under rotary oscillation. *Comput. Fluids*, 26, 755, 1997.
- [4]. S. Choi, K. Choi and S. Kang. Characteristics of flow over a rotationally oscillating cylinder at low Reynolds number. *Phys. of Fluids*, 14(8), 2767, 2002.
- [5]. Hartlen, R. T. and Currie, I. G. Lift-Oscillator Model of Vortex-Induced Vibrations. *Journal of Engineering Mechanics*, 96(5), 577, 1970.
- [6]. A. H. Nayfeh, F. Owis and M.R. Hajj. A model for the coupled lift and drag on a circular cylinder. *Proc. of DETC 2003, ASME 19th Biennial Conference on Mechanical Vibrations and Noise, Chicago, IL, USA, DETC2003/VIB-48455*, 2003.
- [7]. Isam Janajreh and Muhammad Hajj. An Analytical Model for the Lift on a Rotationally Oscillating Cylinder. *BBA VI International Colloquium on: Bluff Bodies Aerodynamics & Applications, Milano, Italy, July, 20–24 2008*
- [8]. Y.C. Kim and E. J. Powers. Digital bispectral analysis and its applications to nonlinear wave interactions. *IEEE Trans. Plasma Sci.*, PS-7 120-131, 1979.
- [9]. M. R. Hajj, R. W. Miksad and E. J. Powers. Fundamental-subharmonic interaction: effect of the phase relation. *Journal of Fluid Mechanics*, 256(403), 1993.
- [10]. M. R. Hajj, R. W. Miksad and E. J. Powers. Perspective: measurements and analysis of nonlinear wave interactions with higher-order spectral moments. *Journal of Fluids Engineering*, 119(3), 1997.
- [11]. E. J. Powers and S. Im. Introduction to higher-order statistical signal processing and its applications. in: *Higher-Order Statistical Signal Processing* (Boashash, Powers & Zoubir eds.) Longman, Australia. 1995.
- [12]. A. H. Nayfeh, *Perturbation Methods* (Wiley, New York. 1973).
- [13]. A. H. Nayfeh, *Introduction to Perturbation Techniques* (Wiley, New York. 1981).